

## Wave Generation in a Numerical Wave Tank

Milad Zabihi K.Kh<sup>1</sup>, Said Mazaheri<sup>2</sup>, Ahmad Rezaee Mazyak<sup>3</sup>

<sup>1</sup>Ph.D. Student, Iranian National Institute of Oceanography and Atmospheric Science; Milad.zabihi88@yahoo.com

<sup>2</sup>Assistant Professor, Iranian National Institute of Oceanography and Atmospheric Science; Said.mazaheri@inio.ac.ir

<sup>3</sup>Ph.D. Student, Tarbiat Modares University; a.rezaemazyak@modares.ac.ir

### Abstract

Developing numerical tanks to study wave structure interaction drew engineers' attention in last decade. Numerical wave tanks are absolutely essential for investigating wave-structure interaction. This paper presents two different numerical software capabilities to generate regular gravity waves in a wave tank. The wave generation was performed using the FLUENT package and Flow-3D. Both models are based on Navier-Stokes and VoF equations. The results of the mentioned models were compared with theoretical results. Free surface elevation and horizontal component of wave particle velocity were the two parameters which have been considered for comparison. Results indicate that Flow-3D in some cases is a bit more accurate than Fluent in capturing free surface elevation. In numerical models it is important to dissipate wave energy and prevent wave reflection. In this way four different slopes were evaluated to determine the minimum slope needed for wave energy dissipation. The results showed that a minimum slope of 1V:35H is needed to avoid wave reflection. The variation of streamlines and velocity potential are also studied. The pattern of horizontal and vertical velocity variation in the fluid domain is similar to stream function and potential velocity function variation, respectively.

**Keywords:** wave tank, numerical, Navier Stokes equation, VOF, regular wave, streamline

### Introduction

Physical model tests in marine laboratories have their own problems such as lack of equipment, expensive instrument and also time consuming process. However, numerical modeling is a good way to study on different phenomena in an efficient manner. Numerical wave tank is an essential part of studying wave structure interaction and recently have been used especially in modeling wave energy converters [1-3]. Predicting wave energy converters efficiency and their response to wave loads are strictly dependent on good modeling of wave behavior and its hydrodynamic characteristics. Hence, during last decade researches made effort to develop numerical wave tanks [4].

Researchers have developed different numerical methods to simulate ocean waves. Wei et al [5] and Chawla [6] implemented a source function method to generate ocean waves, based on Boussinesq model. Based on the 2D form of Navier-Stokes equations, Dong and Huang [7] established a 2D numerical wave tank to simulate small-amplitude waves and solitary waves. Lu [8] numerically simulated wave overtopping against seawalls in regular wave case.

In this paper two numerical models called Fluent and Flow-3D were used for generating regular airy wave. Both models solve Navier-Stokes and VoF equations for two incompressible fluids. It should be noted that VoF model is served to track surface between air and water. The results regarding to free surface elevation and horizontal component of wave particle velocity are compared with theoretical values. All numerical wave tanks need to have a dissipation zone to prevent wave reflection and its subsequent problems. Hence in this paper, it is tried to dissipate wave energy similar to what happens in nature, using mild slope. Four different slopes are tested and the results are presented.

### Background

Before involving numerical simulation it is necessary to have a concise review on linear wave theory formulation and governing equations of the mentioned problem.

- Linear Wave Theory

The most elementary wave theory is the small-amplitude or linear wave theory. This theory, developed by Airy [9], is easy to apply, and gives a reasonable approximation of wave characteristics for a wide range of wave parameters. As just free surface elevation and horizontal component of fluid velocity were the parameters of interest in this paper, their formula are given according to linear wave theory. For further information of other formulas or linear wave theory assumption refer to CEM [10].

$$\eta = \frac{H}{2} \cos(kx - \omega t) \quad (1)$$

$$u = \frac{H}{2} \frac{gT}{L} \frac{\cosh(2\pi(z+d)/L)}{\cosh(2\pi d/L)} \cos(kx - \omega t) \quad (2)$$

$$w = \frac{H}{2} \frac{gT}{L} \frac{\sinh(2\pi(z+d)/L)}{\cosh(2\pi d/L)} \sin(kx - \omega t) \quad (3)$$

where  $\eta$  is free surface elevation.  $H$  is wave height.  $K$  is wave number and  $\omega$  is wave frequency.  $x$  shows the position and  $t$  shows the time. In formula 2 and 3,  $T$  is wave period,  $L$  is wave length,  $d$  is water depth,  $z$  shows the level where velocity is computed and  $g$  is gravity acceleration.

- Governing Equations

Both Fluent and Flow-3D solve Navier-Stokes and Continuity equation. The governing equations in these models are expressed as follows:

- Navier Stokes Equation

Navier-Stokes equation in three dimensional coordination is as follows;

$$\frac{\partial u}{\partial t} + u \frac{\partial u}{\partial x} + v \frac{\partial u}{\partial y} + w \frac{\partial u}{\partial z} = -\frac{1}{\rho} \frac{\partial p}{\partial x} + g_x + \nu \left( \frac{\partial^2 u}{\partial x^2} + \frac{\partial^2 u}{\partial y^2} + \frac{\partial^2 u}{\partial z^2} \right) \quad (4)$$

$$\frac{\partial v}{\partial t} + u \frac{\partial v}{\partial x} + v \frac{\partial v}{\partial y} + w \frac{\partial v}{\partial z} = -\frac{1}{\rho} \frac{\partial p}{\partial y} + g_y + \nu \left( \frac{\partial^2 v}{\partial x^2} + \frac{\partial^2 v}{\partial y^2} + \frac{\partial^2 v}{\partial z^2} \right) \quad (5)$$

$$\frac{\partial w}{\partial t} + u \frac{\partial w}{\partial x} + v \frac{\partial w}{\partial y} + w \frac{\partial w}{\partial z} = -\frac{1}{\rho} \frac{\partial p}{\partial z} + g_z + \nu \left( \frac{\partial^2 w}{\partial x^2} + \frac{\partial^2 w}{\partial y^2} + \frac{\partial^2 w}{\partial z^2} \right) \quad (6)$$

where,  $u$ ,  $v$  and  $w$  are components of velocity field in  $x$ ,  $y$  and  $z$  direction, respectively.  $P$  is the pressure and  $\rho$  is density.  $\nu$  is the kinematic viscosity and  $g_x$ ,  $g_y$  and  $g_z$  are the gravitational acceleration components.

However, assuming  $z$  is in gravity direction,  $g_x$  and  $g_y$  are equal to zero and  $g_z$  will be equal to  $-g$ .

- Continuity Equation

Equation 7 presents the continuity equation and equation 8 shows the continuity equation for incompressible flow.

$$\frac{\partial}{\partial x}(\rho u) + \frac{\partial}{\partial y}(\rho v) + \frac{\partial}{\partial z}(\rho w) + \frac{\partial \rho}{\partial t} = 0 \quad (7)$$

$$\frac{\partial u}{\partial x} + \frac{\partial v}{\partial y} + \frac{\partial w}{\partial z} = 0 \quad (8)$$

All parameters have been introduced following Navier-Stokes equation in previous section.

- VoF Method

As in this paper it is focused on wave generation, consequently free surface capture is an indispensable part of this study. Hence, for surface tracking VoF method has been used. Hirt [11] developed the Volume of fluid (VOF) method to solve the two-phase problem. The VOF formulation is based on the fact that two or more phases are immiscible. In each control volume, the sum of the volume fraction of all phases is unit (Equation (9)). If the  $q$ -th fluid volume fraction is recognized as  $\alpha_q$ , then depending on  $\alpha_q$  value the following three conditions are possible:  $\alpha_q = 0$  shows that the volume is empty of  $q$ -th fluid,  $\alpha_q = 1$  shows that the volume is full of  $q$ -th fluid and any other value between 0 and 1 shows the interface. Hence the continuity equation is as follows: (Equation (10)) [12].

$$\sum_{q=1}^n \alpha_q = 1 \quad (9)$$

$$\frac{1}{\rho_q} \left[ \frac{\partial}{\partial t} (\alpha_q \rho_q) + \nabla \cdot (\alpha_q \rho_q \vec{v}_q) \right] = S_{aq} + \sum_{p=1}^n (\dot{m}_{pq} - \dot{m}_{qp}) \quad (10)$$

where  $\dot{m}_{pq}$  and  $\dot{m}_{qp}$  are the mass transfer of phase  $p$  to  $q$  and vice versa.  $S_{aq}$  is the source term which is zero here.

- Boundary Condition

As mentioned before, a wave tank is needed for wave generation. Hence, the boundary condition of the wave tank is considered as follows; the left hand side of the tank is regarded as velocity inlet. In the upper part atmospheric pressure is applied. The right hand side and bottom of the wave flume is considered as wall boundary condition where no slip condition enforced at walls (normal velocity component is set to be zero).

It should be mentioned that kinematic free surface boundary condition and dynamic free surface boundary condition which are presented as follows are satisfied using VoF in Fluent and Flow-3D software.

If wave free surface is represented according to  $z = \eta(x, y, t)$ , then kinematic free surface wave boundary condition is considered as:

$$w = \frac{\partial \eta}{\partial t} + u \frac{\partial \eta}{\partial x} + v \frac{\partial \eta}{\partial y} \quad (11)$$

Dynamic free surface boundary condition is essential to be applied to illustrate pressure distribution over this boundary.

$$-\frac{\partial \varphi}{\partial t} + \frac{1}{2}(u^2 + w^2) + \frac{P}{\rho} + gz = C(t) \quad (12)$$

### Numerical Wave Tank Characteristics

The numerical wave tank dimension has been introduced in this section. "Figure 1" shows a schematic representation of numerical wave tank and the boundary condition which were implemented. Reflection occurrence is a critical issue which should be considered through wave simulation. In physical modeling, wave energy will be dissipated using porous material in the end of the wave flume. In numerical approach there is also several methods for example using coarser mesh or using a longer flume. Another way is to use a porous zone. In this paper, a sloping beach is considered similar to what happens in real beach. Sloping beach has the merit of investigating wave breaking on slope.

In this paper four mild slopes considered according to "Figure 1" and "Table 1". Two numerical models called Fluent and Flow-3D have been used for wave generation. Wave characteristics were considered equal in both Fluent and Flow-3D models and are presented in "Table 2".

In both models  $dx=0.35$  m is considered along numerical wave tank length except over the slope where it has been equal to 0.45 meter. Vertical elements were variable also, so that finer mesh was applied near still water level where the variation of water level and capturing free surface level was important. Near SWL  $dy=0.005$  meter was used. The generated mesh for case 1 is shown in "Figure 2" as an example.

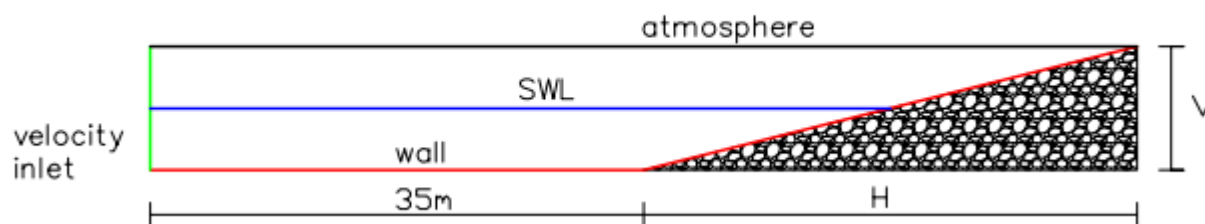


Figure 1: A schematic of numerical wave tank

Table 1: Four different cases considered for numerical beach slope

Slope Characteristics	Case 1	Case 2	Case 3	Case 4
V	1	1	1	1
H	5	20	35	50

Table 2: Wave characteristics

Wave characteristics		
H	d (SWL over bottom)	T
0.1m	0.6m	2s

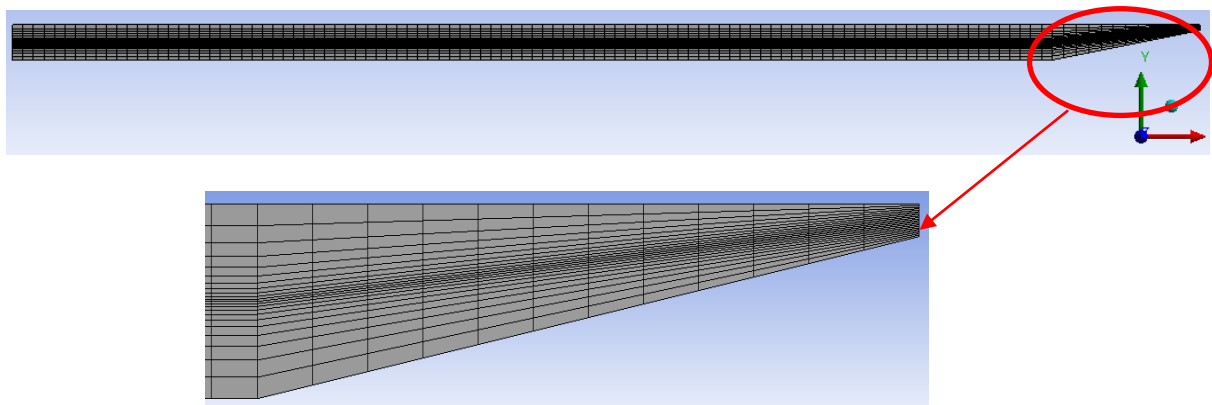


Figure 2: Numerical wave tank meshing, slope 1V:5H

### Results and Discussion

The result of free surface elevation has been compared using Flow-3D, Fluent and linear wave theory. The comparison has been performed for four slopes introduced in "Table 1". To ensure that wave generation is fully developed the comparison has been performed after 30 seconds of wave generation. It should be mentioned that free surface elevation has been captured for  $x=12m$  from wave maker which is approximately equal to 3 times of wave length. "Figure 3" to "Figure 6" show the results. As it is obvious in all Figures, Fluent results have a phase difference with those theoretical ones which is the result of initial condition. However, it can be understood from the results that Fluent results are more accurate especially in wave crest capturing (See "Figure 5").

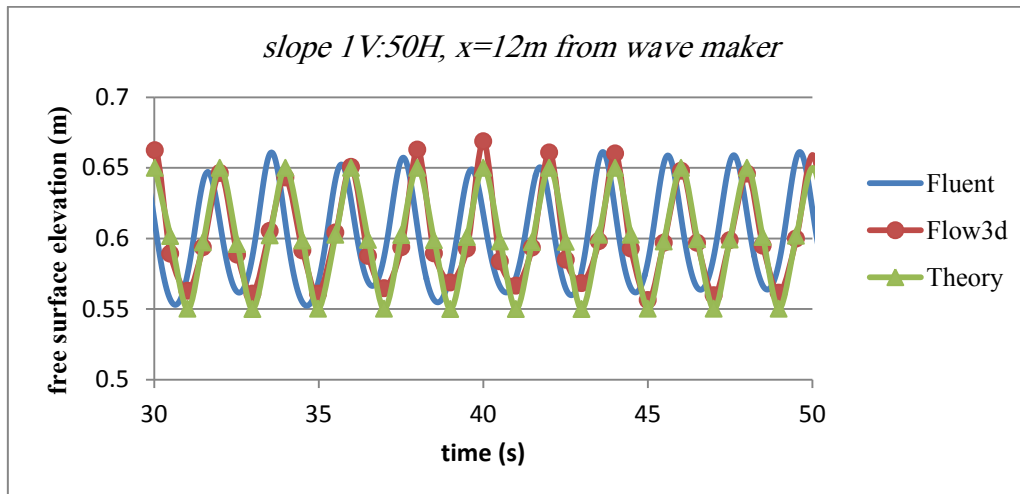


Figure 3: Comparison of free surface elevation for slope 1V:50H

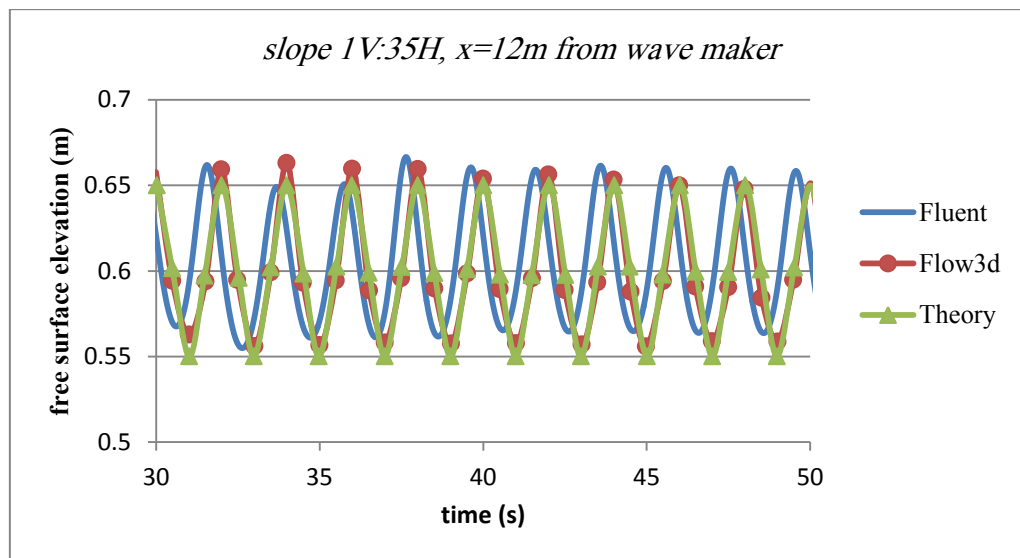


Figure 4: Comparison of free surface elevation for slope 1V:35H

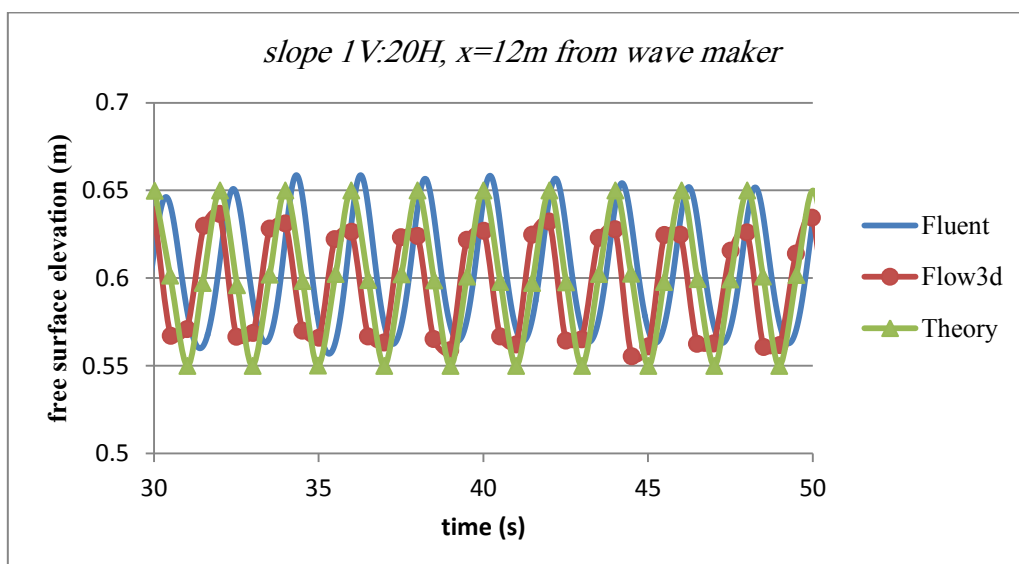


Figure 5: Comparison of free surface elevation for slope 1V:20H

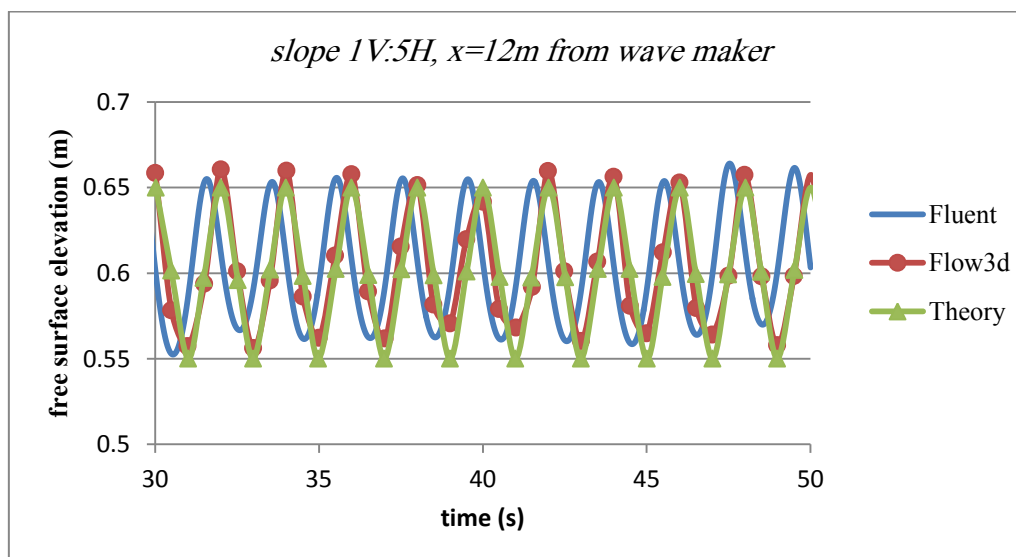


Figure 6: Comparison of free surface elevation for slope 1V:5H

"Table 3" shows statistical comparison of Fluent and Flow-3D output with theoretical results. Root mean square error (RMSE) has been used as an index of comparison. The RMSE formula is given in equation (13). The results are according to four different slopes which were introduced in "Table 1". "Table 3" shows that Flow-3D results are less deviated from theoretical results comparing to Fluent outputs.

$$RMSE = \sqrt{\frac{1}{N} \sum_{i=1}^N (y_{Numerical} - y_{theory})^2} \quad (13)$$

Table 3: Statistical comparison of Fluent and Flow-3D

RMSE for point x=12m	Fluent	Flow-3D
Case 1	0.043	0.016
Case 2	0.029	0.024
Case 3	0.039	0.014
Case 4	0.039	0.016

In the second stage wave profile has been captured just before the slope; x=35 meter from wave maker, using both Fluent and Flow-3D. "Figure 7" and "Figure 8" show the results of Fluent and Flow-3D models, respectively. It is easily understood from "Figure 7" that slope 1V:50H and 1V:35H ensure wave profile follows linear wave theory pattern, where crest and trough of the wave are between 0.65 and 0.55m. It is also clear that wave profile at point x=35m is influenced more when slope 1V:5H is tested.

"Figure 8" shows the simulation results obtained by Flow-3D. It is visible that wave profile is influenced more by the slope 1V:5H and 1V:20H due to wave reflection occurrence. From these two Figures it can be said, minimum required slope to dissipate wave energy and consequently to prevent wave reflection is 1V:35H within the range of this paper tests.

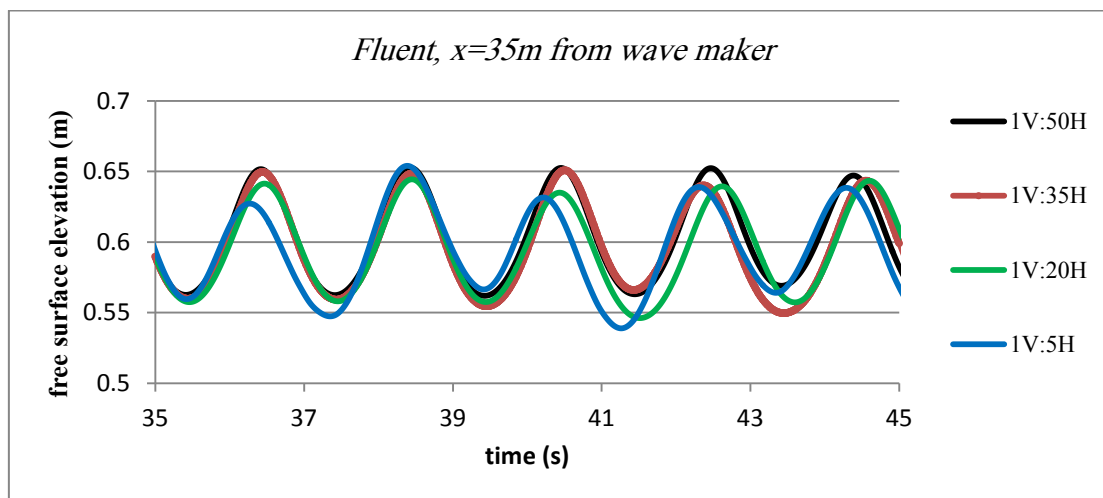


Figure 7: Comparison of free surface elevation at  $x=35\text{m}$  for different slopes, Fluent

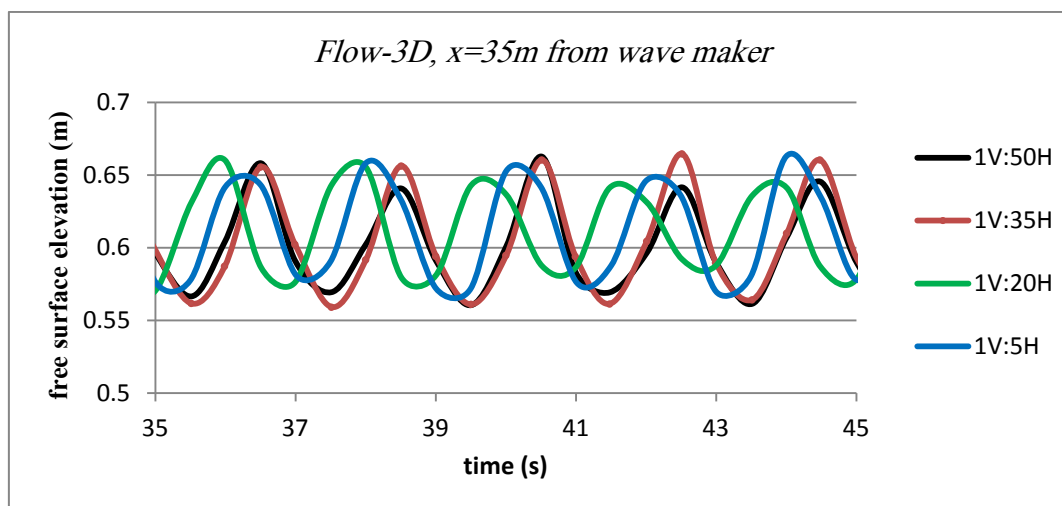


Figure 8: Comparison of free surface elevation for at  $x=35\text{m}$  for different slopes, Flow-3D

Wave horizontal velocity is the second parameter evaluated for different beach slopes. As it is seen, "Figure 9", wave horizontal velocity at  $x=20\text{m}$  is not influenced by slope 1V:35H and 1V:50H. In fact, wave reflection effect is considerable for slope 1V:20H. Hence, similar to aforementioned explanation, a minimum slope of 1V:35H is essential to prevent wave reflection in fluid domain.

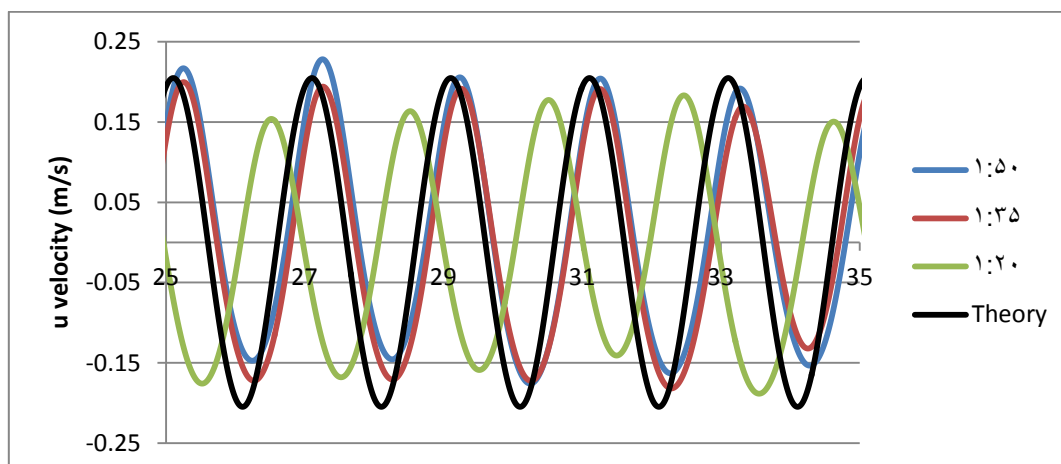


Figure 9: Comparison of wave horizontal velocity for different slopes

The wave horizontal and vertical velocity variation in fluid domain are shown in "Figure 10". Comparing "Figure 10" and "Figure 11", it can be understood that the pattern of horizontal velocity variation is similar to streamlines and the pattern of vertical velocity variation is similar to the velocity potential. This concept can be explained as follows; Stream function according to linear wave theory can be defined as follows:

$$\psi = \frac{a\omega}{k} \frac{\sinh(k(z+d))}{\sinh(kd)} \cos(kx - \omega t) \quad (14)$$

where  $a$  is amplitude of wave height,  $k$  is wave number,  $\omega$  is frequency,  $z$  is the position relative to still water level and  $d$  is the water depth. Again, we know that;

$$u = \frac{\partial \psi}{\partial z} = a\omega \frac{\cosh(k(z+d))}{\sinh(kd)} \cos(kx - \omega t) \quad (15)$$

Hence,

$$\frac{\psi}{u} = \frac{\sinh(k(z+d))}{k \cosh(k(z+d))} \Rightarrow \psi = \frac{\sinh(k(z+d))}{k \cosh(k(z+d))} u = \frac{\tanh(k(z+d))}{k} u \quad (16)$$

Asymptotic forms of hyperbolic function according to [13 and 14] are shown in Table 4 and Eqs (17-19).

Table 4 asymptotic form of hyperbolic function [13]

Function	Large $Kh$	Small $Kh$
Cosh $kh$	$e^{kh}/2$	1
Sinh $kh$	$e^{kh}/2$	$kh$
Tanh $kh$	1	$kh$

$$\text{deep water} = \frac{\cosh(k(z+d))}{\sinh(kd)} = \frac{\sinh(k(z+d))}{\sinh(kd)} = e^{kz} \quad (17)$$

$$\text{shallow water} = \frac{\cosh(k(z+d))}{\sinh(kd)} = \frac{1}{kd} \quad (18)$$

$$\frac{\sinh(k(z+d))}{\sinh(kd)} = 1 + \frac{z}{d} \quad (19)$$

For deep water condition (large  $Kh$ ), similar to Eq 16, stream function is as follows;

$$\psi = \frac{\sinh(k(z+d))}{k \cosh(k(z+d))} u = \frac{e^{k(d+z)}}{ke^{k(d+z)}} u = \frac{1}{k} u \quad (20)$$

For shallow water condition (small  $Kh$ ), stream function is as follows;

$$\psi = \frac{\sinh(k(z+d))}{k \cosh(k(z+d))} u = \frac{k(d+z)}{k} u = (d+z)u \quad (21)$$

According to Eqs 20 and 21, it is visible that variation of horizontal velocity can show the pattern of streamline variation. Based on this approach, in deep water condition, the ratio of horizontal velocity to wave number shows the stream function and in shallow water condition, the stream function can be obtained using Eq 21. Similar to aforementioned Eqs, the relation between vertical velocity and potential velocity function can be calculated.

$$\phi = \frac{a\omega}{k} \frac{\cosh(k(z+d))}{\sinh(kd)} \sin(kx - \omega t) \quad (22)$$

$$v = \frac{\partial \phi}{\partial z} = a\omega \frac{\sinh(k(z+d))}{\sinh(kd)} \sin(kx - \omega t) \quad (23)$$

$$\frac{\phi}{v} = \frac{\cosh(k(z+d))}{k \sinh(k(z+d))} \Rightarrow \phi = \frac{\cosh(k(z+d))}{k \sinh(k(z+d))} v = \frac{\tanh(k(d+z))}{k} v \quad (24)$$

Again, using "Table 4" and Eqs (17-19) the relation between vertical velocity and potential velocity function is obtained for deep (Eq 25) and shallow (Eq 26) water condition.

$$\phi = \frac{\cosh(k(z+d))}{k \sinh(k(z+d))} v = \frac{1}{k} v \quad (25)$$

$$\phi = \frac{\cosh(k(z+d))}{k \sinh(k(z+d))} v = \frac{k(d+z)}{k} v = (d+z)v \Rightarrow \phi \propto v \quad (26)$$

In brief, it can be said that in linear wave theory; horizontal velocity is proportional to stream function and the vertical component of wave velocity is proportional to potential velocity function. Hence, the pattern of horizontal and vertical velocity variation in the fluid domain is similar to stream function and potential velocity function variation, respectively (See "Figure 10" and "Figure 11").

As it is shown in "Figure 12", the variation pattern of horizontal component of wave velocity before reflecting from slope (t=20s) is similar to "Figure 13". As the time passes reflection occurs (t=50s) and the velocity pattern will change.

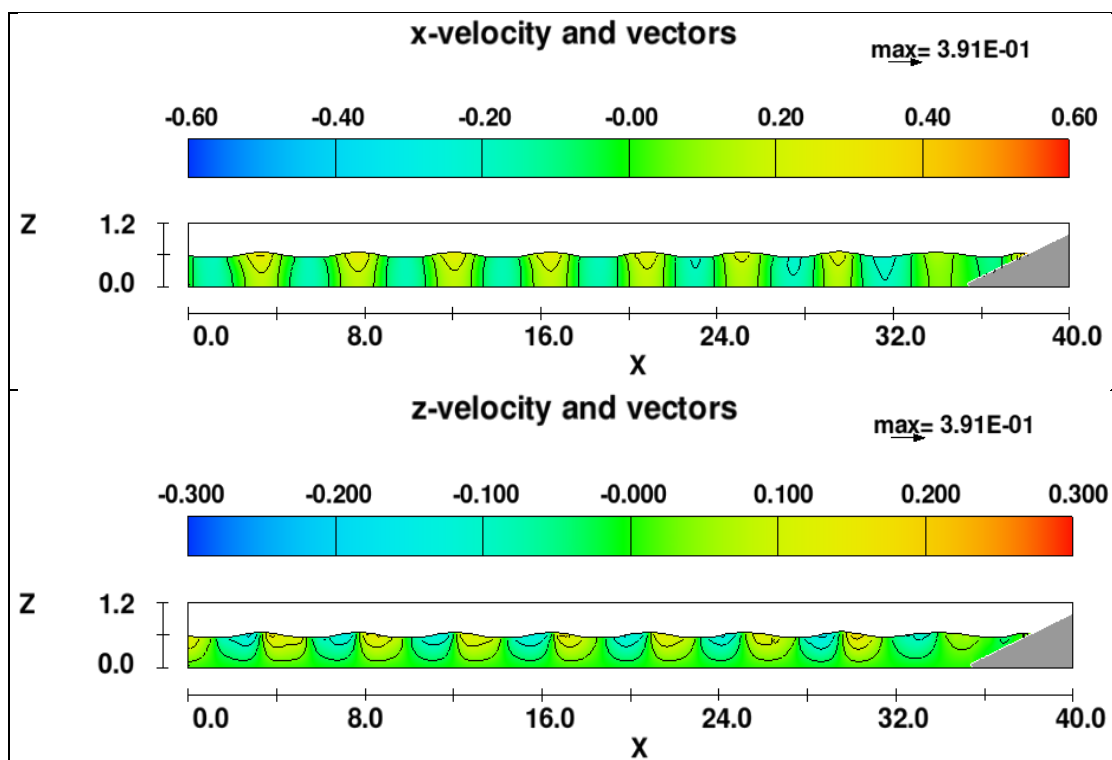


Figure 10: Horizontal and vertical velocity variation in fluid domain

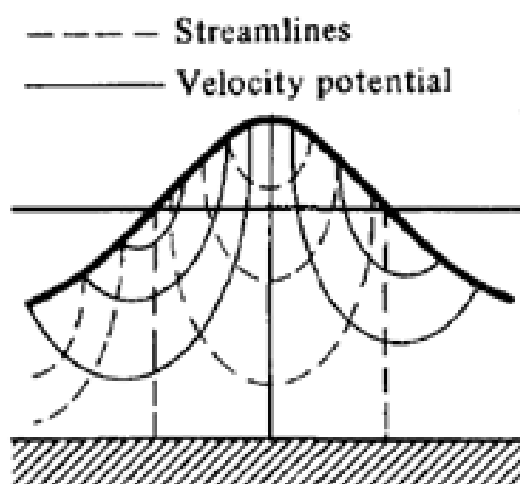


Figure 11: Streamlines and velocity potentials for a progressive wave [13]



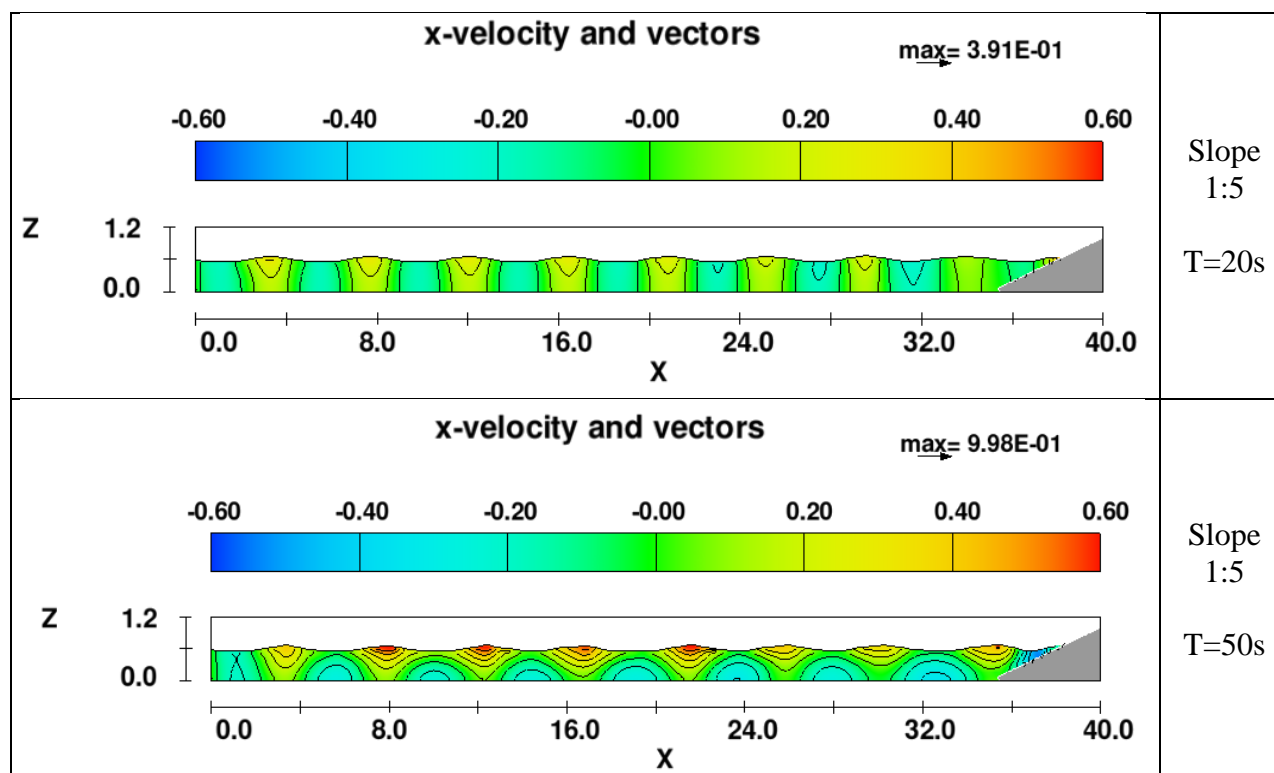


Figure 12: horizontal velocity variation in fluid domain at t=20s and t=50s

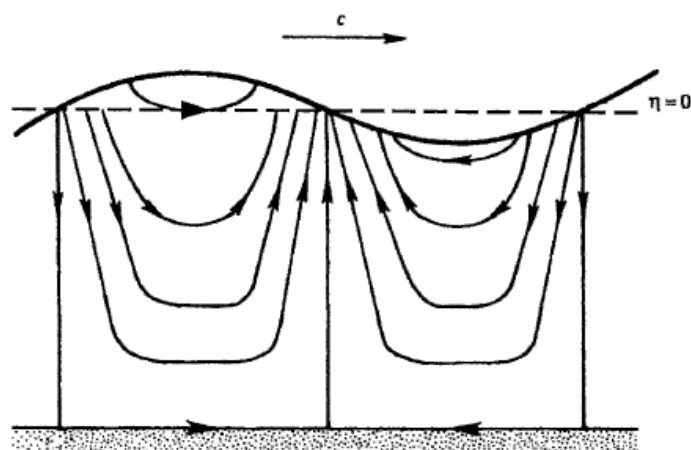


Figure 13: Streamlines pattern for a progressive wave [13]

According to simulation made by Flow-3D software, shown in "Figure 14", the greater the beach slope is, the more reflection occurs and consequently streamlines will undergo more variation than that of shown in "Figure 13". According to "Figure 14", it should be noted that the pattern of horizontal velocity variation is different in each of four considered slopes and the most variation takes place in wave breaking time. Hence, future studies will be dedicated to obtain wave reflection coefficient so that a quantitative analysis of fluid domain will be performed besides qualitative illustration.

### Summary and Conclusion

Numerical wave tanks are essential part of wave structure interaction modeling and are served as a platform in nowadays researches, especially in evaluation of wave energy devices efficiency or hydraulic response of marine structures. In this paper two numerical models called Fluent and Flow-3D were used to generate regular waves in a numerical wave tank. The capability of these two models in wave generation was analyzed by comparing theoretical surface elevation and numerical results. The results of the two models were similar; however, Fluent results had slight phase difference with theoretical results. To obtain a minimum slope needed for preventing wave reflection, four different slopes were considered and the surface elevation just at the toe of the slope as well as wave horizontal velocity in  $x=20\text{m}$  were monitored. The results showed that within the range of this paper, a minimum slope of 1V:35H is sufficient to avoid wave reflection in fluid domain.

The streamlines and velocity potential pattern also were obtained through simulation via Flow-3D numerical model. The variation of the streamlines in different slopes and especially in breaking time were shown. The pattern of

horizontal and vertical velocity variation in the fluid domain is similar to stream function and potential velocity function variation, respectively. Finally, both numerical models showed having powerful tools in wave generation problem. Future study will be focused on wave reflection determining which leads to fluid domain analysis both quantitatively and qualitatively.

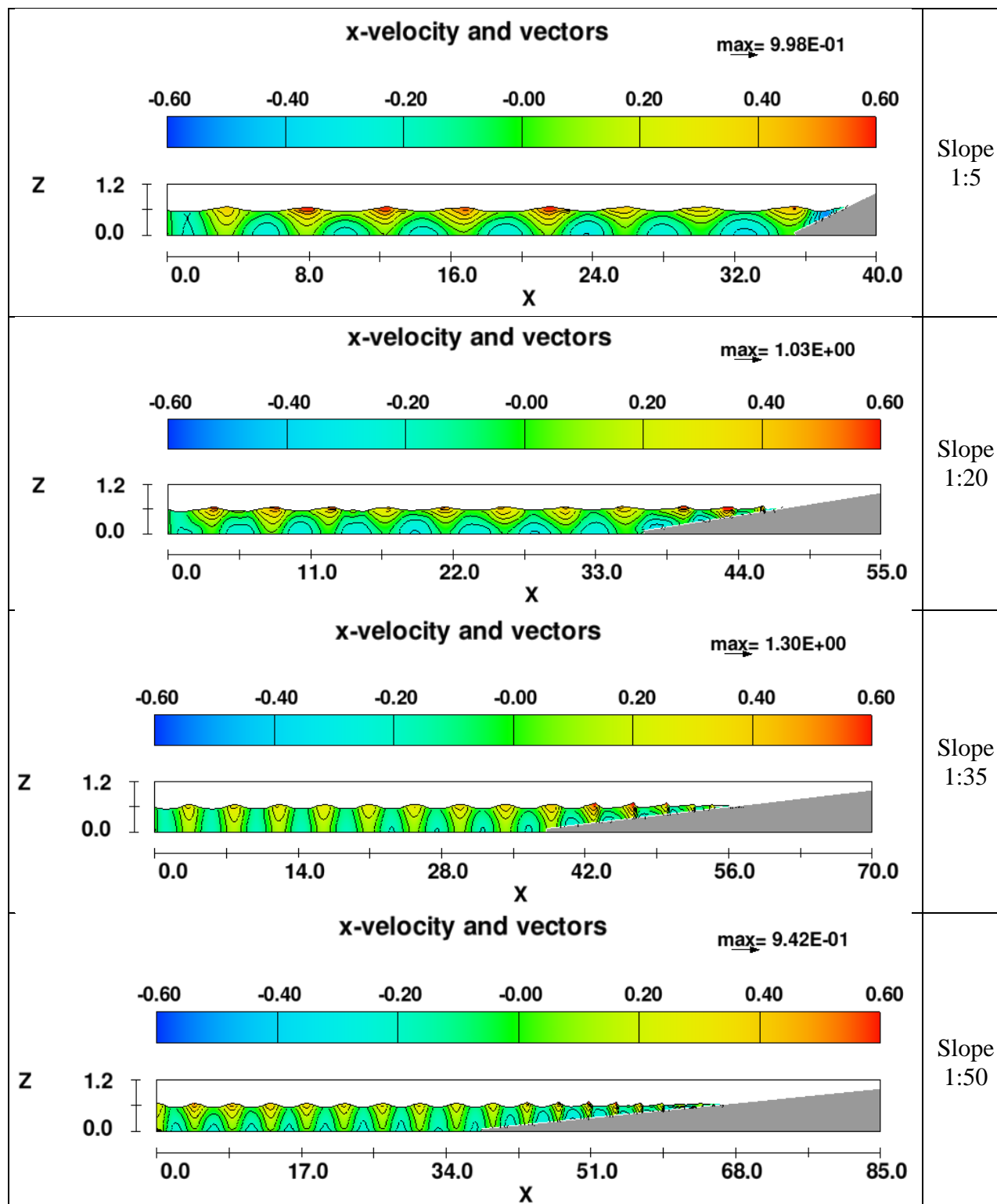


Figure 14: Comparison of horizontal velocity variation in fluid domain for different slopes

## References

- [1] Horko, M., "CFD Optimization of an Oscillating Water Column Wave Energy Converter," University of Western Australia, 2008.
- [2] Bouali, B. and Larbi, S., "Contribution to the Geometry Optimization of an Oscillating Water Column Wave Energy Converter," *Energy Procedia*, 36, 565-573, 2013.
- [3] Teixeira, P. R., Davyt, D. P., Didier, E. and Ramalhais, R., "Numerical simulation of an oscillating water column device using a code based on Navier–Stokes equations," *Energy*, 61, 513-530, 2013.
- [4] Qingjie, Du., Dennis, Y. C., Leung., "2D numerical simulation of ocean waves," *World Renewable Energy Congress*, Sweden, 2011.
- [5] Wei, G., Kirby, J.T. and Sinha, A., "Generation of waves in Boussinesq models using a source function method," *Coastal Engineering*. 36(4): pp. 271-299, 1999.
- [6] Chawla, A. and Kirby, J.T., "A source function method for generation of waves on currents in Boussinesq models," *Applied Ocean Research*. 22(2): pp. 75-83, 2000.
- [7] Dong, C.M. and Huang, C. J., "Generation and propagation of water waves in a two-dimensional numerical viscous wave flume," *Journal of Waterway, Port, Coastal and Ocean Engineering*. 130(3): pp. 143-153, 2004.
- [8] Lu, Y.j., "Numerical simulation of two-dimensional overtopping against seawalls armored with artificial units in regular waves," *Journal of Hydrodynamics*, 19( 3): pp. 322-329, 2007.
- [9] Airy, G. B. "Tides and Waves," *Encyc. Metrop.*, Article 192, pp 241-396, 1845.
- [10] *Coastal Engineering Manual (CEM)*, US Army Corps of Engineering, 2006
- [11] Hirt, C.W. and B.D. Nichols, "Volume of fluid (VOF) method for the dynamics of free boundaries," *Journal of Computational Physics*,. 39(1): pp. 201-225, 1981.
- [12] Gomesa, M. N., Olinto, C. R., Rocha, L. A. O., Souza, J. A. and Isoldi, L. A., "Computational modeling of a regular wave tank," *Thermal Engineering*, Vol. 8, p. 44-50, 2009.
- [13] Dean, R.G. and Dalrymple, R. A., "Water wave mechanics for engineers and scientists," 1984.
- [14] Sorensen, R. (1997). *Basic Coastal Engineering*, Springer US